

General Disclaimer

One or more of the Following Statements may affect this Document

- This document has been reproduced from the best copy furnished by the organizational source. It is being released in the interest of making available as much information as possible.
- This document may contain data, which exceeds the sheet parameters. It was furnished in this condition by the organizational source and is the best copy available.
- This document may contain tone-on-tone or color graphs, charts and/or pictures, which have been reproduced in black and white.
- This document is paginated as submitted by the original source.
- Portions of this document are not fully legible due to the historical nature of some of the material. However, it is the best reproduction available from the original submission.

DOE/JPL-956797/01

9950-936

JPL Contract No. 956797

QR-10092-01

EXCIMER LASER ANNEALING TO FABRICATE LOW COST SOLAR CELLS

(NASA-CR-173938) EXCIMER LASER ANNEALING TO
FABRICATE LOW COST SOLAR CELLS Quarterly
Technical Report, 26 Mar. - 30 Jun. 1984

N84-34027

(Spie Corp., Bedford, Mass.) 37 p

HC A03/MF A01 CSCJ

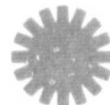
(Spire Corp., Bedford, Mass.) 37 p Unclassified
HC A03/MF A01 CSCL 10A G3/44 23919

Digitized by srujanika@gmail.com

CSCL 10A G3/44 23919

Quarterly Technical Report No. 1
July 1984

JET PROPULSION LABORATORY
CALIFORNIA INSTITUTE OF TECHNOLOGY
PASADENA, CALIFORNIA 91109



spire

QR-10092-01
July 1984

EXCIMER LASER ANNEALING TO
FABRICATE LOW COST SOLAR CELLS

Quarterly Technical Report No. 01
For Period Covering 26 March to 30 June 1984

Contract No. 956797

Jet Propulsion Laboratory
Flat-Plate Solar Array Project
Module Performance and Failure Analysis Area

Approved by: Anton Greenwald
Anton C. Greenwald, Principal Investigator

Approved by: M.B. Spitzer
Mark B. Spitzer, Program Manager

SPIRE CORPORATION
Patriots Park
Bedford, Massachusetts 01730

TABLE OF CONTENTS

<u>Section</u>		<u>Page</u>
1	INTRODUCTION	1-1
2	TECHNICAL PROGRESS	2-1
2.1	Task (1)(A): Select Process	2-1
2.2	Task (1)(B): Assess Effect of Process Variables	2-2
2.2.1	Optical Equipment	2-4
2.2.2	Optimization of Front Junction Parameters	2-6
2.3	Task (3)(A): Preliminary Cost Analysis	2-15
2.3.1	Solar Cell Ion Implanter	2-17
2.3.2	Pulsed Excimer Laser Annealer	2-17
2.3.3	Process Sequence Comparison	2-24
2.4	Other Tasks	2-24
3	CONCLUSIONS AND RECOMMENDATIONS	3-1
4	PLANNED WORK IN THE NEXT REPORTING PERIOD	4-1
5	REFERENCES	5-1

LIST OF ILLUSTRATIONS

<u>Number</u>		<u>Page</u>
1	Experimental Laser Annealing Station	2-5
2a	Optical Microphotograph of Edge of (Darker) Anneal Pattern on Polished Wafer 4520-1	2-9
2b	Sem Microphotograph of Edge of Texture Etched Wafer 4519-2 after PELA	2-9
3	Higher Magnification Microphotographs of Texture-Etched Wafer 4519-2	2-9
4a	Wafer 4519-3 after PELA, 0.020" Step	2-11
4b	Wafer 4519-7 after PELA, 0.035" Step	2-11
5	Schematic Diagram of Junction Depth Variation Seen from Groove and Stain Measurement on Wafer 4520-14	2-14
6a	External Quantum Efficiency of Cell 4520-5a	2-16
6b	External Quantum Efficiency of Cell 4520-1a	2-16
7	SPI [®] ION 1000 Solar Cell Ion Implanter	2-18
8	Scanning Pattern for Annealing a 100 cm ² Square Wafer	2-21
9	Program Schedule	4-2

LIST OF TABLES

<u>Number</u>		<u>Page</u>
1	Process Sequence Comparison	1-2
2	Pulse Excimer Laser Anneal	2-7
3	Process Sequence Comparison	2-23

ABSTRACT

The objective of this research is to show whether or not pulsed excimer laser annealing (PELA) of ion-implanted junctions is a cost effective replacement for diffused junctions in fabricating crystalline silicon solar cells. The preliminary economic analysis completed during the first quarter of this program shows that the use of PELA to fabricate both the front junction and back surface field (BSF) would cost approximately 35¢ per peak watt (Wp), compared to a cost of 15¢/Wp for diffusion, aluminum BSF and an extra cleaning step in the baseline process described by JPL. The cost advantage of the PELA process depends on improving the average cell efficiency from 14% to 16%, which would lower the overall cost of the module by about 15¢/Wp.

The technical goal of this research is to develop an optimized PELA process compatible with commercial production, and to demonstrate increased cell efficiency with sufficient product for adequate statistical analysis. During the first quarter of this program an excimer laser annealing station was set-up and made operational. The first experiment used 248 nm radiation to anneal phosphorus implants in polished and texture-etched silicon. Preliminary results showed that the PELA processed cells had overall efficiencies comparable to furnace annealed ion implanted controls, and that texture-etched material requires lower fluence for annealing than polished silicon. Process optimization will be carried out in the second quarter.

SECTION I INTRODUCTION

The objective of this research is to show whether or not pulsed excimer laser annealing (PELA) of ion implanted junctions is a cost effective replacement for diffused junctions in fabricating silicon solar cells. Required experiments and analysis are described below.

The first task (1A) is to select a process group which has functional equivalency to the baseline process group defined by JPL. The choice of Spire Corporation is shown in Table 1. Ion implantation and laser annealing will be used in place of diffusion of phosphorus for the front junction, and in place of aluminum drive-in for the back surface field.

The second task (1B) is to assess the sensitivity of the selected process to all significant input variables. Past published work has reduced the number of variables which must be optimized to produce a good cell. Emphasis is placed on determining the upper and lower limits on laser fluence and overlap of successive pulses for annealing of high dose, low energy phosphorus ion implantation. This junction formation technique is to be applied to texture-etched material to which screen printed contacts will later be applied. It is necessary to examine the resultant shallow, highly doped junctions, to determine if such structures which contribute to high efficiency solar cells, are consistent with commercial screen printing contact formation processes.

The third task (1C) investigates the suitability and efficiency of the specific excimer laser selected for this application. It is expected that the results of task (1B) will show whether or not a 50 watt laser with wavelength of either 308 or 248 nm is sufficient to anneal a 10 cm x 10 cm silicon wafer in less than six seconds.

The fourth task (1D) is to demonstrate the achievement of a process cost reduction by producing a quantity of cells utilizing the proposed process group. The planned demonstration will fabricate 300 solar cells 100mm in diameter, plus controls, using the

equipment identified for production use, although full automation will not be used. The average cell efficiency and yield of this demonstration will be used in calculating the cost of this process.

The fifth task (3A) is to perform a preliminary economic analysis of the selected excimer laser process compared with competing technologies. The results in the first quarter indicate that ion implantation and PELA of both front and back surfaces of a wafer would cost about twice as much as the equivalent baseline process group. However, since the PELA process is expected to result in more efficient cells, significant cost savings can still be realized. If the technical results of this program show that the back implant and anneal are not needed, then the cost savings would be almost \$0.32/peak watt.

The sixth task (3B) is a final economic analysis of this process using the yield and efficiency data of the demonstration experiment (Task 1C). This experiment will include furnace annealed controls and an economic comparison between PELA and furnace annealing will be included.

TABLE I
PROCESS SEQUENCE COMPARISON

BASELINE	PELA
DIFFUSE JUNCTION	IMPLANT FRONT
ALUMINUM BSF	IMPLANT BACK*
CLEAN	ANNEAL FRONT ANNEAL BACK*

* Back implant and anneal may not be necessary.

SECTION 2 TECHNICAL PROGRESS

2.1 TASK (I) (A): SELECT PROCESS

The process chosen for the application of excimer lasers to the fabrication of silicon solar cells consists of non-mass-analyzed (NMA) ion implantation of (a) phosphorus for the front junction and (b) boron for the back surface field (BSF) followed by (c) pulsed excimer laser annealing (PELA) of both sides. This PELA process replaces the following steps in the baseline process outlined by JPL and shown in Table I: diffusion of the junction, application of aluminum and drive-in to form the back surface field, and finally a cleaning step.

The choice of this process is based upon past work at Spire Corporation on ion implantation, furnace annealing and pulse annealing to fabricate silicon solar cells, and the published work of Young et al.⁽¹⁾ The best solar cell reported formed by excimer laser annealing has AM1 efficiency of 16.7%. The structure comprises a p⁺nn⁺ doping and was formed by PELA of a glow discharge implant of BF₃ into n-type silicon.⁽¹⁾ The best ion implanted silicon solar cells (18% efficiency at AM1) comprised an n⁺pp⁺ doping formed by a furnace annealed phosphorus implant.⁽²⁾ Since best results^(2,3) thus far have been obtained with a phosphorus implant, the choice was made to use primarily phosphorus in the present work. Young et al reported testing only boron and arsenic, and not phosphorus implants when they optimized their PELA process.⁽⁴⁾ An additional consideration militating for use of phosphorus implants in p-type wafers was that most production silicon solar cells are n⁺pp⁺. Thus, our choice made the process consistent with potential commercial users.

NMA implantation was chosen for economic reasons. Spire Corporation has shown that NMA implantation yields cells that perform as well as conventional mass-analyzed ion implanted cells.⁽⁵⁾ There is, however, an economic advantage when NMA sources are used owing to the significantly higher beam currents that can be generated for the same size ion source and accelerator. The work of Young et al⁽¹⁾ shows that BF₃ gas can be used in such an accelerator for the BSF; but at this time diborane (B₂H₆) is also being considered.

Spire Corporation has chosen to work with 1 to 2 ohm-cm p-type silicon based upon cost and past yield. Lower resistivity material does not produce good solar cells unless SiO_2 surface passivation is used; however, Spire's SiO_2 passivation process does not appear to be compatible with PELA. Thus, at present, low resistivity Si was not selected. Higher resistivity material is sensitive to the quality of the back surface field (BSF). The effect of a BSF in 1 to 2 ohm-cm silicon, however, is minimal and the boron implant could probably be deleted from the process. However, Spire has found that back boron implants improve the back contact in very high efficiency solar cells. The effect of this implant on the overall economics of cell fabrication will be determined as part of this program.

Spire Corporation recently conducted a review of rapid annealing technologies.⁽⁶⁾ Excimer laser annealing has significant advantages over other pulsed laser methods for the fabrication of high efficiency cells. The production of beam by the excimer laser and the utilization of beam energy during annealing are more efficient than other forms of laser annealing. The beam is more uniform on a macroscopic scale than the beam produced by other types of lasers and consequently does not need an homogenizer. The beam is also more uniform on a microscopic scale since its coherence is not as great as in for example Q-switched lasers, and does not show minute diffraction effects which lead to hot spots and defects in the silicon junction region. Newer model excimer lasers are rugged and have the precise power control required for production.

In summary, Spire Corporation has chosen NMA ion implantation and PELA as the experimental process to replace the equivalent process group of diffusion and the aluminum BSF steps in the baseline process. This choice and its technical justification completes Task 1A.

2.2 TASK (1) (B): ASSESS EFFECT OF PROCESS VARIABLES

The objective of this task is to determine the sensitivity of the selected process, PELA of ion implanted junctions, to all significant process parameters. These parameters include laser wavelength, pulse width, beam uniformity, fluence and percentage overlap as well as sample surface preparation, implanted ion type, ion dose, ion energy, sample temperature and atmosphere. Those parameters which are considered fixed in light of previous results are discussed first.

As mentioned in Section 2.1, previous studies on pulsed annealing ion-implanted solar cells have shown that an optimized front junction implant is $^{31}\text{P}^+$ at 10 keV, 7 to 10 degrees off axis, at room temperature, with a dose uniformity of ± 10 percent at 2.5×10^{15} ions/cm.⁽³⁾ At higher implant energies (25 keV) the junction depth is increased while lower energies increase the cost of implantation owing to reduced beam currents. The same studies have shown that the implant of BF_2^- for a back surface field is optimized at 25 keV, 2.5×10^{15} ions/cm², same angle, and similar uniformity requirements. Lower energies again reduce beam current while higher energies increase the tail depth of implanted boron beyond what would be melted by the laser. A change in these parameters is not anticipated at this time. Note that all ion doses are increased for texture - etched material to account for the increase in surface area.

Previous PELA studies have shown the effect of variations in laser pulse width and microscopic beam uniformity.⁽⁷⁾ The laser chosen for our work has a fixed pulse width of 20 ns which is near optimum for minimizing the fluence required. Examination of the surface has revealed no microscopic defects which would damage the cell. Diffractions patterns from dust or surface defects that are seen with Q-switched ruby or Nd-Yag lasers⁽⁸⁾ are not found in material irradiated with excimer lasers.

Process simplification for production applications requires that annealing be performed in air at room temperature. Pulsed laser annealing with Nd-Yag lasers is sensitive to sample temperature, but no temperature effect has been observed with excimer lasers.⁽⁷⁾ Pulsed laser annealing in air can result in the growth of a very thin oxide surface film, about 5nm thick. The film is not passivating and it is not expected to affect screen printed contacts or AR coating requirements. The PELA process should be performed under a laminar air flow hood with filters to preclude dust that might interfere with annealing.

This study emphasizes the effect of the laser wavelength, fluence, and overlap on polished or texture-etched wafers with phosphorus or boron implants. The work was broken up into five subtasks:

- 1) Setting up the optical equipment.
- 2) Optimizing parameters to anneal phosphorus implants in polished surfaces (front junction).
- 3) Optimizing parameters to anneal phosphorus implants in texture - etched surfaces.
- 4) Optimizing parameters for screen printed contacts.
- 5) Optimizing parameters for fabricating the back surface field (BSF).

The goal of each subtask and the work accomplished during the first quarter of this contract is summarized below.

2.2.1 Optical Equipment

At the start of this program a suitable excimer laser was available but the required optics and sample positioning equipment were not. Thus it was necessary to assemble sample-handling equipment and this was done in the second month of the contract. A schematic diagram of the set up is shown in Figure 1. To assure fixed positioning between the focusing lens and the sample, all parts were mounted on an optical breadboard. The cylindrical lens and mirror were specifically fabricated and coated for use at either 248 nm or 308 nm. Slightly improved performance could be expected if the lenses are coated for one fixed wavelength. The optics, mountings, and positioners were attached to an optical table which could be stabilized in a vertical position. The focal point of the laser is held fixed while the sample moves; this assures a constant beam profile and fluence for a fixed laser output. The x-y translation stage has a linear accuracy of 0.0005 in./in. of travel, a positional repeatability of 0.002 in., and a total travel of 5 inches in either direction. More accurate tables can be purchased but are not necessary. The table is driven by stepper motors, motor drivers, and a microprocessor controller. Minimum step size is 0.001 inch and maximum speed is 8000 steps per second (20 cm/sec). The microprocessor controller was chosen because it contains internal relays which can be used directly to trigger the laser. Other positioning controllers could not trigger the laser and therefore required a second process controller to synchronize the equipment.

ORIGINAL PAGE IS
OF POOR QUALITY

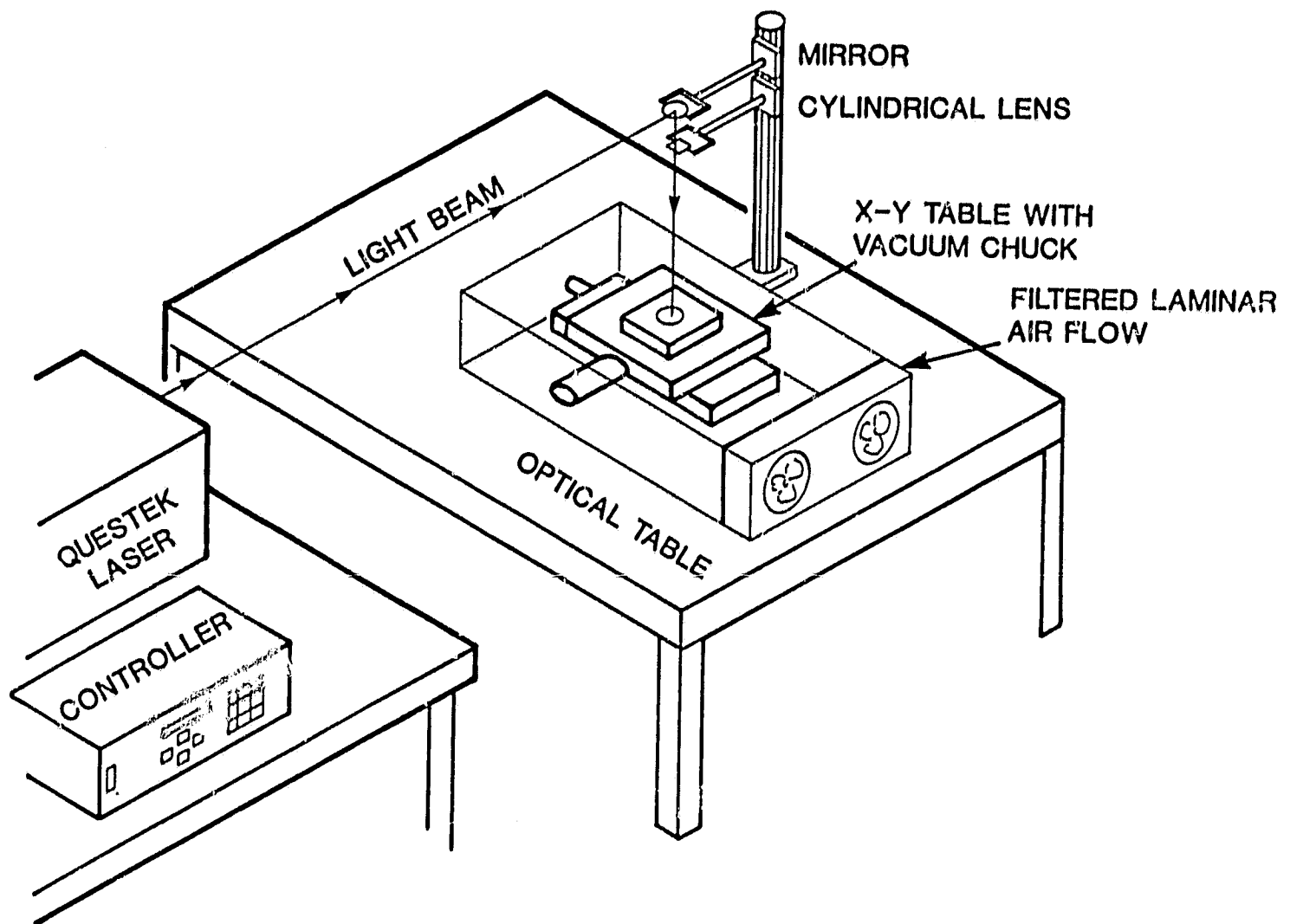


FIGURE 1. EXPERIMENTAL LASER ANNEALING STATION

A standard Questek laser was used for this work (designated model number 2200-2). The beam size at the laser aperture is 1.0 inch x 0.5 inch, with the long dimension horizontal. Typical power with XeCl is 400 mJ per pulse. The output is measured on each pulse. The laser electronics are controlled by a microprocessor and typical output variations from pulse to pulse were ± 5 mJ out of 400, which is better than the specification for this laser.

2.2.2 Optimization of Front Junction Parameters

Experiments on subtask 2 for polished surfaces and experiments on subtask 3 for texture-etched surfaces were conducted in parallel. The starting material was float zone p-type silicon with a resistivity of 1.5 ohm-cm (100) orientation with one flat. One lot of 15 wafers (lot # 4520) was cleaned and implanted with phosphorus at 10 keV to a dose of 2.5×10^{15} ions/cm². The backs of these wafers had etched surfaces. A second lot of identical material (lot # 4519) was first texture-etched on both sides with an average pyramid height of 1 to 3 microns (see Figure 3a). The front surface was then implanted with phosphorus at 10 keV to a dose of 4.3×10^{15} ions/cm². The dose was calculated to give equal doping levels in both types of surfaces. After implantation about half of the wafers in each lot were annealed by the pulsed excimer laser.

For the initial experiments the laser was filled with krypton, HCl, and neon gas. The x-y table controller was not able to trigger the laser (later corrected) which was run in a manual control mode without the excimer laser Powerlok™ feature which stabilizes the beam output. With a new gas fill the initial beam output was 500 mJ which gradually diminished to 450 mJ as the gas was conditioned. The power output stabilized at this lower level. Beam power was measured before and after processing each wafer, average power is noted in Table 2. The wavelength of the beam was 248 nm.

TABLE 2. PULSE EXCIMER LASER ANNEAL

CELL	VOC (mV)	Jsc (mA/cm ²)	FF (%)	EFF. (%)	SHEET	APPROX FLUENCE (J/cm ²)	ENERGY (mJ)	STEP SIZE (Inches)	FOCA WIDTH (mm)
4519 Textured									
2	---	---	---	---	41	1.7	496	.020	1
3a	570	22.85	70.7	9.21	33	1.6	477	.020	1
3b	565	22.73	62.6	8.04	33	1.6	477	.020	1
4a	568	22.64	63.5	8.16	32	1.5	448	.010	1
4b	532	21.98	41.9	4.90	32	1.5	448	.010	1
5	---	---	---	---	--	1.0	300	.020	1
6a	552	25.97	75.1	10.77	46	1.0	300	.020	1
6b	537	26.67	72.5	10.38	46	1.0	300	.020	1
7a	537	26.03	75.3	10.53	47	0.75	448	.035	2
7b	527	26.89	73.9	10.46	47	0.75	448	.035	2
8a	583	29.46	75.3	12.93	70			Furnace annealed control	
8b	581	29.75	73.2	12.65	70			Furnace annealed control	
4520 Polished									
1a	559	22.58	72.2	9.09	46	1.65	496	.020	1
1b	537	21.34	67.4	7.73	46	1.65	496	.020	1
2a	552	22.56	71.3	8.89	46	1.6	490	.020	1
2b	545	22.43	66.8	8.17	46	1.6	490	.020	1
3a	552	22.27	70.0	8.61	43	1.5	457	.010	1
3b	552	22.45	70.4	8.73	43	1.5	457	.010	1
4a	534	23.76	70.2	8.91	65	1.0	300	.020	1
4b	552	23.43	66.4	8.12	65	1.0	300	.020	1
5a	550	22.39	73.7	9.07	70			Furnace annealed control	
5b	550	22.68	72.9	9.09	70			Furnace annealed control	
13a	537	22.89	68.9	8.47	57	0.74	444	.025	2
13b	519	22.70	68.0	8.01	57	0.74	444	.025	2
14	---	---	---	---	--	0.74	444	.035	2
15a	550	22.15	73.1	8.91	49	1.55	4.67	.010	1
15b	540	22.07	67.3	8.02	49	1.55	4.67	.010	1

• No AR Coating

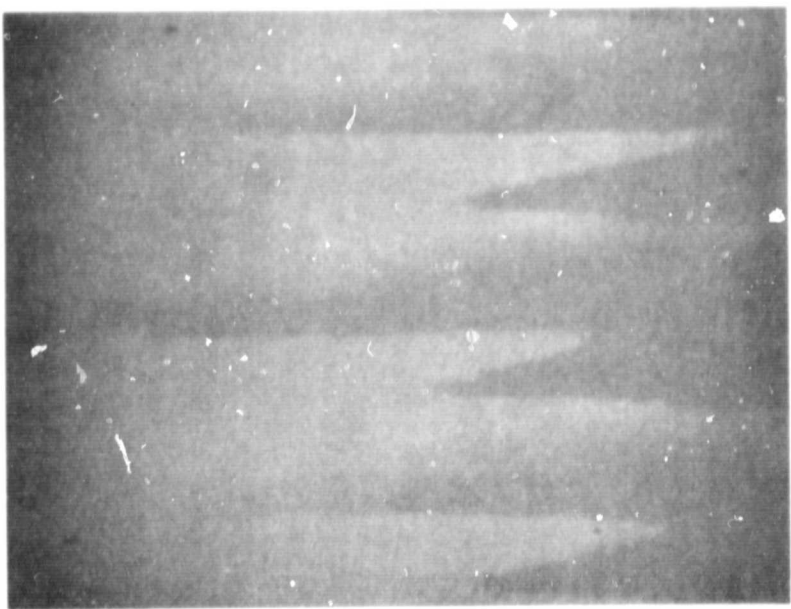
The focal point of the cylindrical lens was initially set to give a beam width of approximately 1.0 mm. The width was determined by measuring the burn mark on a piece of paper. However, the fluence across the width of the beam was non-uniform, being greater in the center than at the edges. As shown in Figure 2b, the most intense portion of the beam was about 0.3 mm wide while the width of the beam which annealed the sample was at 0.7 mm and possibly 0.9 mm wide. The non-uniformity in fluence made measurement impossible at that time. Numbers quoted in Table 2 are averages; total energy divided by beam area (30 mm by either 1 or 2 mm).

The laser beam was not collimated in the direction perpendicular to the focal line. The length of the original beam (25 mm) expanded to an annealed length on the wafer of about 30 mm, and a maximum length of visible effect of 40 mm. As shown in Figure 2 on a polished wafer, the anneal pattern at the edge of the beam consists of "spikes" at the beam center, plus regions where the beam overlap was sufficient to alter the material in two pulses. The silicon surface exposed to low fluence irradiation may be (a) unaltered from the amorphous phase created by high dose ion implantation, (b) crystallized into a very fine grain material that was never melted, or (c) melted to only a shallow depth and characterized by grains about 100 nm long. In all of these cases, melting the silicon surface to the proper depth at the correct fluence will complete a satisfactory anneal of the ion implant damage. This is assured with sufficient overlap.

The overlap in the long direction was 10 percent. The pattern was moved 25 mm (1.0 inch) between two successive series of scans overlapping the 30 mm spot size by 2.5 mm. The overlap in the short direction was about 50 percent. The wafer was moved 0.5 mm (0.020 inch) between successive pulses so that all areas would be pulsed at least twice with a 1.0 mm wide beam. This parameter was varied during the experiment.

There was no visible pattern left by PELA on polished wafers fully annealed. Only at the edge of the beam could a pattern be discerned (Figure 2a). However, the step size could easily be seen in texture-etched material, as shown in Figure 4. The reason for this was easily discerned by SEM examination. At low magnification, Figure 2b, the pattern of wide bright stripes and thin dark bands seen optically (Figure 4) is reversed.

ORIGINAL PAGE IS
OF POOR QUALITY



← ANNEALED BY
OVERLAPPING
PULSES

← BEAM CENTER

↑
BEAM WIDTH
↓

FIGURE 2 a. OPTICAL MICROPHOTOGRAPH OF EDGE OF (DARKER) ANNEAL PATTERN ON POLISHED WAFER 4520-1 (52x)

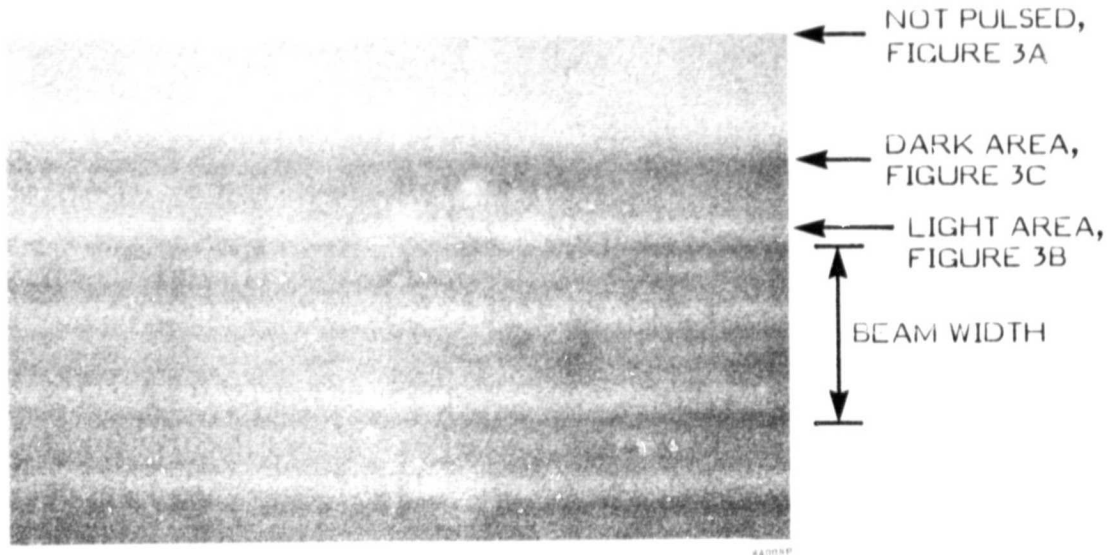
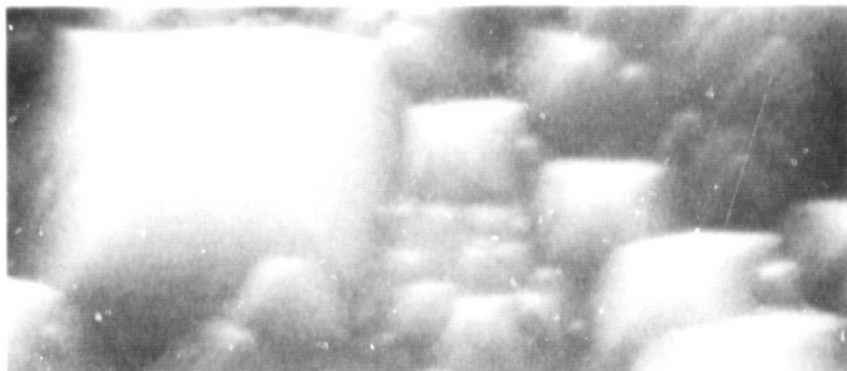


FIGURE 2b. SEM MICROPHOTOGRAPH OF TEXTURE-ETCHED WAFER 4519-2 AFTER PELA

ORIGINAL PAGE IS
OF POOR QUALITY.



(A) AFTER IMPLANT



(B) PELA, LIGHT AREA
IN FIGURE 2b



(C) PELA, DARK AREA
IN FIGURE 2b

30 kV 09.1 kX — 1 μ 0016 6-25-84

FIGURE 3. HIGHER MAGNIFICATION MICROPHOTOGRAPHS
OF TEXTURE - ETCHED WAFER 4519-2 (Figure 2b)

OVERLAP REGION

ORIGINAL PAGE IS
OF POOR QUALITY

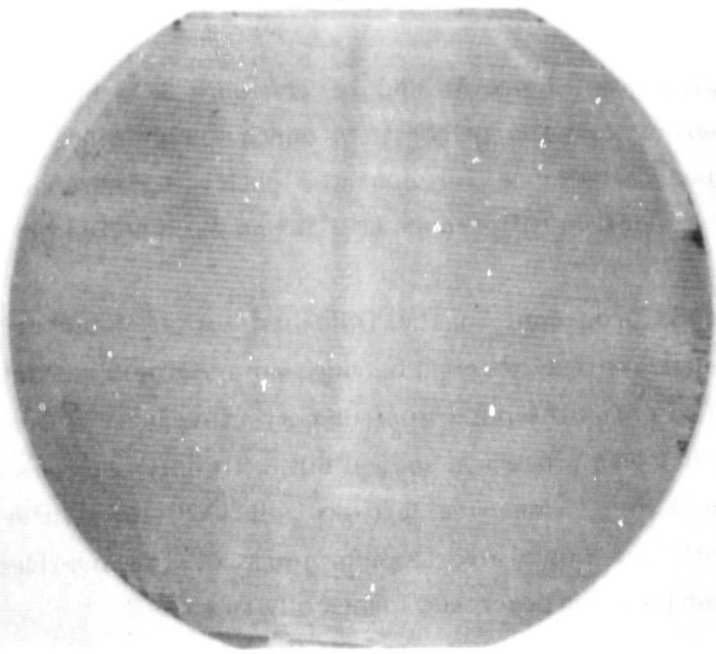


FIGURE 4a WAFER 4519-3 AFTER PELA, 0.020" STEP

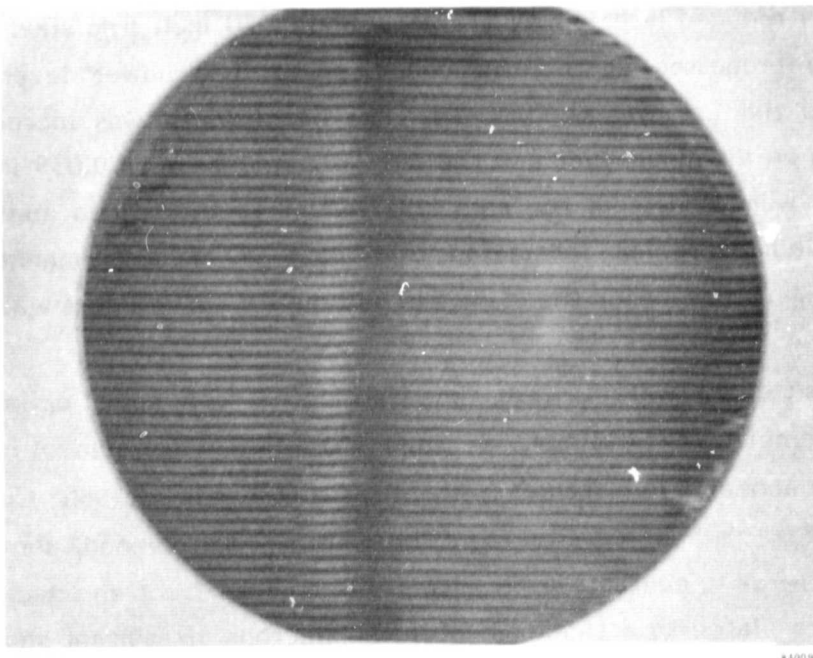


FIGURE 4b WAFER 4519-7 AFTER PELA, 0.035" STEP

At higher magnification (Figure 3b and 3c) the dark SEM bands appear to be smoother, more heavily melted than the bright SEM bands (compare to Figure 2a). As the first surface has higher reflectance for light the optical appearance is explained. Why the reverse is seen for electron reflectance at a 30° angle in an SEM is not clear.

Wafers were processed in the following order: Number 4519-2 was first, but annealing was halted halfway through because an asymmetrical pattern was visible. This sample was used to check the pattern after correcting laser optics and was not made into cells. Wafer 4520-1 was processed second but with only one pass of the laser so that an unannealed strip 4 mm wide was left on cell 4520-16. Wafer 4520-2 was annealed similarly but with the beam overlapping, most of the overlapped area was on cell 4520-2b. Wafer 4519-3 was processed identically to 4520-2.

Experimental parameters were then varied, increasing overlap to 75%, reducing fluence by one-third, then increasing the focused beam by a factor of two and increasing the step size at the same time. Wafers 4520-15, 4520-3, and 4519-4 were processed in that order with the same beam conditions as before, but a step size of only 0.010 inch (about 0.025 mm). The next wafer 4519-5 broke in transit and was used to check optics when using a reduced laser power (Table I) and 0.020 inch step size. Wafers 4520-4 and 4519-6 were processed at this reduced fluence. The power level of the laser now stabilized as the gas was conditioned. The beam width was increased to 2.0 mm as measured on an aluminum disc and the step size increased to 0.035 inch. Wafers 4519-7 and 4520-14 were annealed, the step size reduced to 0.025 inch and wafer 4520-13 was annealed. Cells were not fabricated from 4520-14 because unannealed regions were visible between steps (hence the change in parameters for the next wafer).

The annealed wafers were now fabricated into solar cells except for three unsuitable samples (4519-2, 4519-5, and 4520-14). Two control wafers, 4519-8 and 4520-5, were annealed in a furnace using a three step process (550° C for 2 hours, 850° C for 15 minutes, 550° C for 2 hours). The wafers were cleaned, photoresist applied and patterned. Ti-Pd-Ag contacts were evaporated on both front and back and sintered. The contacts were plated to a thickness of seven microns. Resultant shadow loss was about 3%. Two 2 x 2 cm cells were sawed from each wafer and the I-V characteristics measured (Table I). The cells were not anti-reflection (AR) coated.

The efficiency of these cells is poor because of a non-ohmic back contact. Aluminum should have been evaporated onto the cell back prior to evaporation of titanium. Comparisons should be made only to the co-processed furnace-annealed controls. Also, a small increase in cell efficiency can be expected if the cell edges are etched to remove dicing saw damage.

The reflectance of the pulsed excimer laser annealed (PELA) cells made from texture-etched material was much greater than the texture-etched furnace annealed controls due to melting of the pyramids. This results from excess laser fluence. (Note that the pyramid height in a commercial wafer is greater, typically 10 microns). The increased reflectance led to V_{oc} and J_{sc} of these PELA cells being closer to the polished control cell parameters than the textured cell. The I-V curves will be remeasured after AR coating to reduce the effect of this variable.

In lot 4520 (polished), the PELA cell 4520-1a is nearly identical to the control cells while several other results (2a, 4a, 15a) are very close. The cells are designated with an "c" and "b" suffix to indicate which side of the wafer they were fabricated from. The fact that nearly all type-b cells were slightly poorer in performance than type-a cells may imply that the overlap at the edge of the beam in the long direction was not optimum. The fact that cells from wafers 2 and 15 were similar to results in wafers 1, 2 and 4 implies that substantial overlapping of the beam pattern in the narrow direction did not degrade cell performance. Cell 1b is unusual in that 20% of the surface was not annealed, yet the power output of this cell was only 15% lower than that of 1a. This area remained unannealed after the low temperature contact sinter (Figure 2a). It is concluded that the high resistance of the unannealed layer is sufficient to prevent shunting of the junction by metal coverage.

Wafer 4520-14, not used to make cells, was grooved and stained for a junction depth measurement. The junction depth showed a periodic variation with a maximum of 0.24 microns in the center of the beam pattern and a minimum of 0.17 microns near the edge. The results did not photograph well and so are shown schematically in Figure 5. Spreading resistance measurements will be made on silicon cut from wafer 4520-1 with the best PELA result.

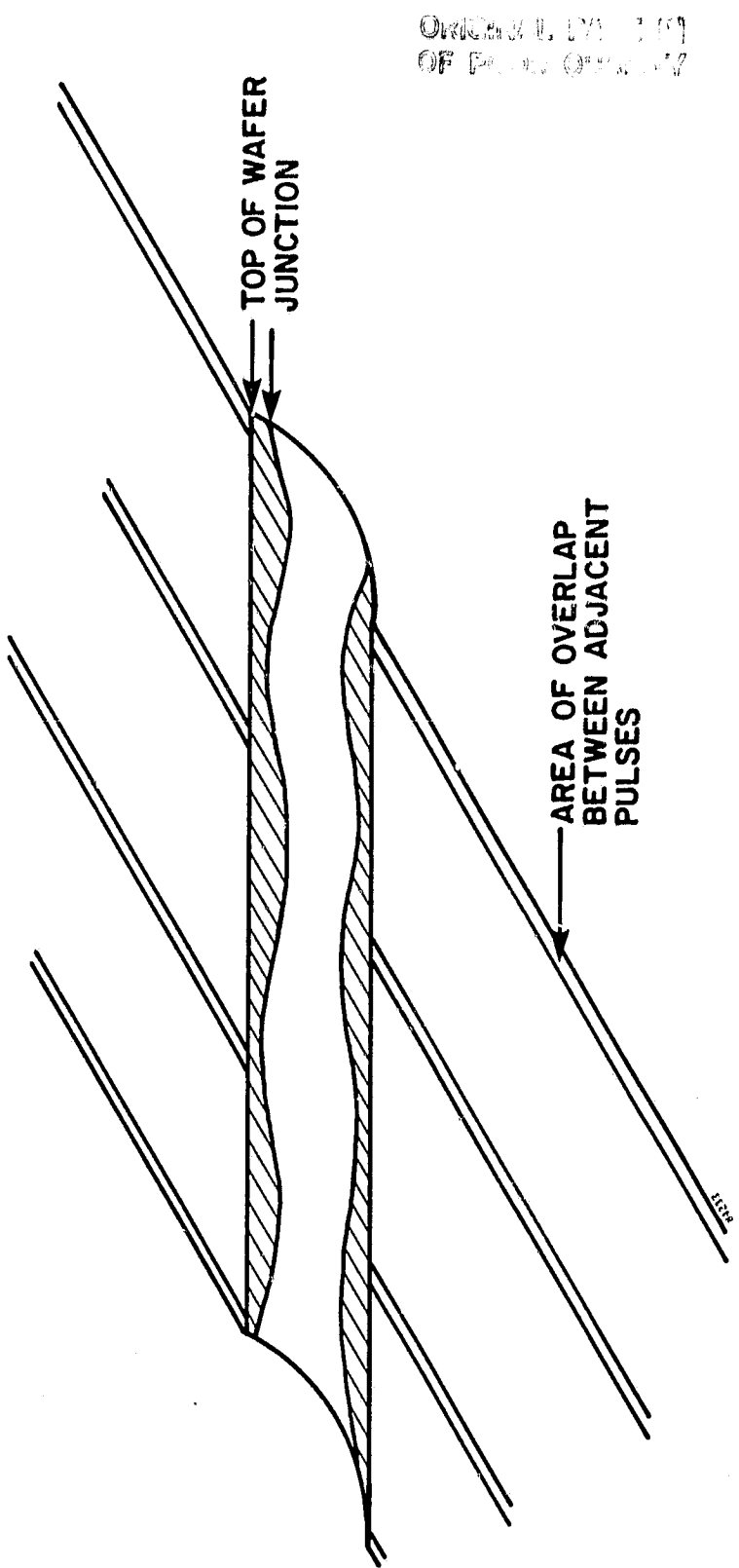


FIGURE 5. SCHEMATIC DIAGRAM OF JUNCTION DEPTH VARIATION SEEN FROM GROOVE AND STAIN MEASUREMENT ON WAFER 4520-14

The sheet resistance of all wafers was measured before processing (Table 2). The extremely low values on wafers 4519-3 and 4519-4 are believed to be due to excessive melting; as the surface area was reduced due to flattening the surface carrier concentration increased. The high value for wafer 4520-14 is due to unannealed thin stripes between the laser pulses. The high resistivity for 4520-4, pulsed at low fluence, could also be due to regions of high resistivity in incompletely annealed material. In this case the poor regions may have been polycrystalline due to insufficient melt depth as opposed to amorphous in wafer 4520-14. The fact that cell 4a was still relatively good implies that PELA is relatively insensitive to fluence and poor overlapping conditions.

Quantum efficiency measurements were made on selected cells. Figure 6a and b show the results for PELA cell 4520-1a and the control cell 4520-5a. The laser annealed cell has poorer blue response and better red response although the differences are small. The difference in blue response is tentatively attributed to a non-optimized junction depth. The improved red response is tentatively attributed to improved carrier lifetime in the base region as the material was not exposed to the high temperatures used on the control cell. Further measurements are needed to test these conclusions.

2.3 TASK (3) (a): PRELIMINARY COST ANALYSIS

In order to assess the reduction in cost achievable with the proposed process sequence we have made a conceptual design of the production equipment needed to produce 5MW per year of 16% efficient cells. The equipment consists of two solar cell ion implanters and two excimer laser annealers, described below, operated by two unskilled persons with 10% of a maintenance technician assigned to each machine.

The input assumptions are:

Throughout : 600 wafer per hour (each machine)
Wafer : 10cm x 10cm sheet silicon with 16% efficient cells.
Cell Power : $.080 \text{ W/cm}^2 \times 100\text{cm}^2 \times 0.16 = 1.28 \text{ watt}$.
Yearly Power : $600 \text{ wafers/hr} \times 1.28 \text{ watt/wafer} \times 0.973 \text{ yield}$
 $\times 0.82 \text{ (fraction uptime)} = 613 \text{ watt/hr}$
 $\times 8280 \text{ hr/yr} = 5.073 \text{ MW/Year}$.

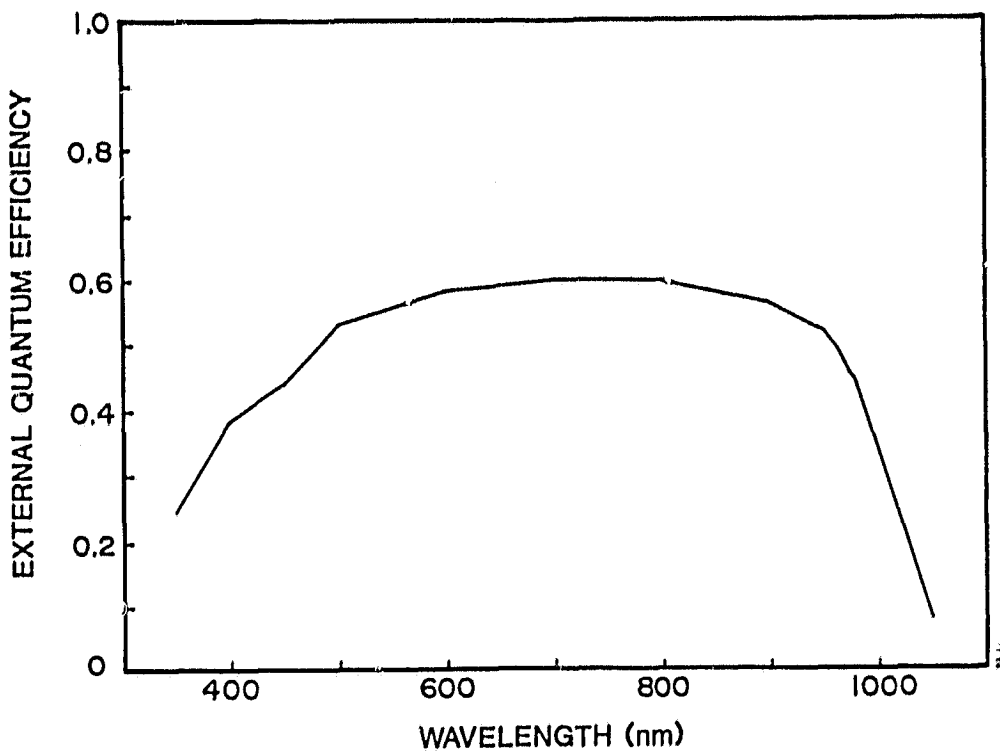


FIGURE 6a. EXTERNAL QUANTUM EFFICIENCY OF CELL 4520-5a

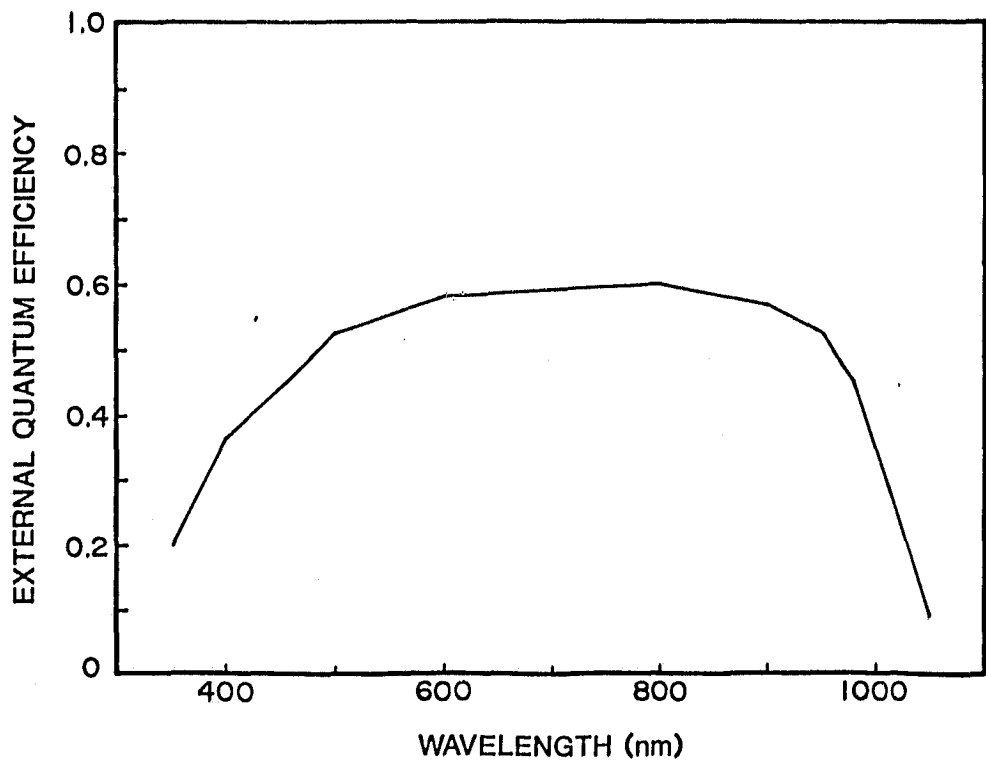


FIGURE 6b. EXTERNAL QUANTUM EFFICIENCY OF CELL 4520-1a

The four machines constitute a balanced line to produce front and back doping at a rate of 5 MW per year with 82% equipment uptime and an overall process step yield of 0.973. This yield is equal to that of the three steps which are being replaced (Section 2.1). The yield should actually be higher since there is no heating or mechanical force on the wafer as in the baseline BSF aluminum print step. However, we are assuming the same yield in order to compute a conservative estimate.

2.3.1 SOLAR CELL ION IMPLANTER

All economic analysis has been done using data on the Spire SPI[®]-ION 1000 solar cell ion implanter. One of these machines will be used to implant the front of the wafers with phosphorus, while a second machine implants the back with BF₃ or B₂H₆. The SPI[®]-ION 1000 is a cassette to cassette non-mass-analyzed ion implanter with a maximum throughput of 600 wafers per hour. On the production line, the operator would flip over the cassette from the output of the first machine before inserting it into the input of the second implanter. A schematic diagram of this machine, and its specifications, are shown in Figure 7.

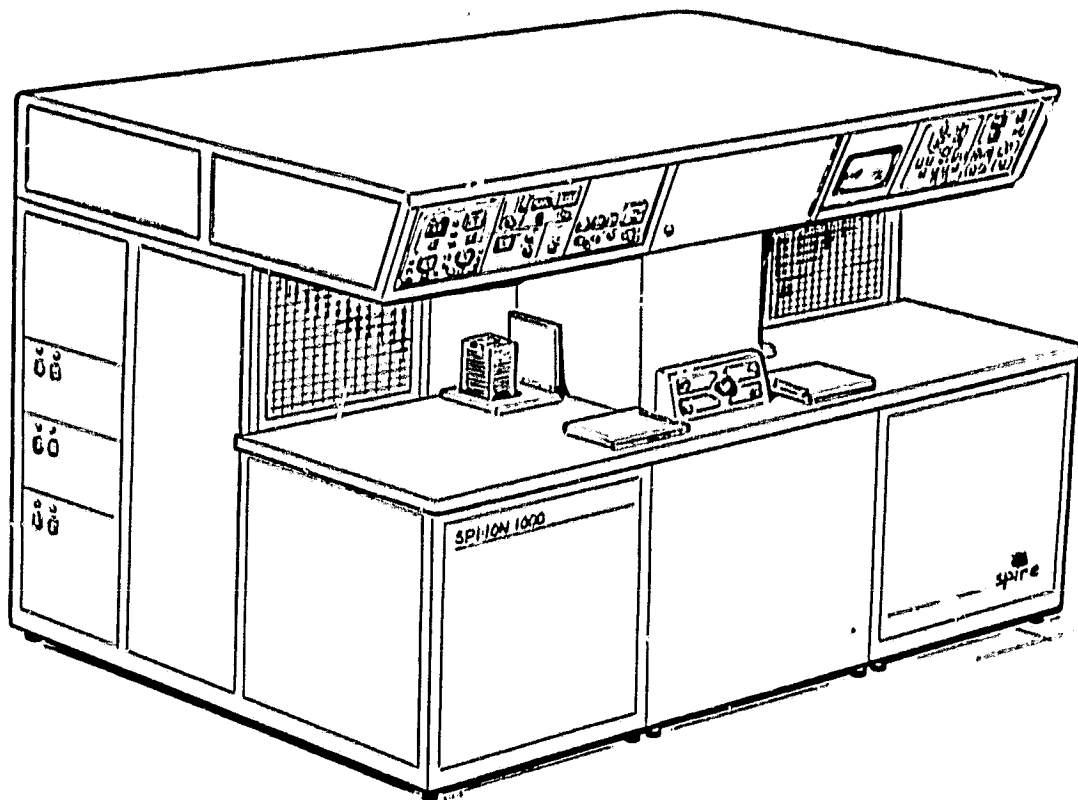
The cell results of non-mass-analyzed ion implantation tests were published by Spire Corporation.⁽⁶⁾ The prototype for the SPI[®]-ION 1000 is nearly complete and undergoing tests. An IPEG analysis for the cost of implantation is given below.

2.3.2 Pulsed Excimer Laser Annealer

The conceptual design of an automated laser annealer is very similar to the experimental system shown in Figure 1 with the addition of an automated cassette loader/unloader. The unloader removes a wafer from the cassette and deposits it on the vacuum chuck. The x-y table then moves the wafer under the laser beam and returns to its starting position. The wafer is lifted from the vacuum chuck and returned to its original position in the cassette which is translated upward (or downward) to the next wafer.

ORIGINAL DRAWING
OF POOR QUALITY

FIGURE 7. SPI-ION 1000 SOLAR CELL ION IMPLANTER



SPECIFICATIONS

Ions	Phosphorus (P_1 , P_2^+) Gases (N ₂ O, Ar, etc.)
Mass Analysis	None
Energy	5-25 keV
Wafer Size	Round or Rectangular 2.5 to 4 inches (60 to 100 mm)
Throughput	600 W/hr @ 5×10^{15} atoms/cm ²
Dose Range	10^{14} - 10^{18} atoms/cm ²
Floor Footprint	88" x 65" (2.25 m x 1.65 m)
Wafer Handling	Cassette-to-Cassette

ION IMPLANTATION COST

<u>EQUIPMENT PRICE</u>	\$630,000 (Including \$30k spare parts)	x 0.59	= \$371,700
<u>FLOOR AREA</u>	50 sq. ft.	x 136	= \$ 6,800
<u>DIRECT LABOR</u>			
1.5 Operator x \$5/hr. x 8280 hrs =	\$ 20,700		
0.1 Maintenance x \$10/hr. x 8280 hrs =	\$ 8,280		
		x 2.02	= \$ 58,540
<u>MATERIALS</u>			
1. Ion source parts \$1500/mo. x 12 =	\$ 18,000		
2. Repair parts at \$1000/mo. x 12 =	\$ 12,000		
3. (a) Phosphorus \$5/day x 345 days/yr =	\$ 1,725		
3. (b) BF ₃ \$115/bottle/wk x 52 wks =	\$ 5,980	x 1.17	=
4. Electricity 10kw x 8280 x \$0.1/kwh =	\$ 8,280		
5. Cooling air and water at 10kw	\$ 8,280	(a)	94,033
6. Liquid nitrogen 100 liters/shift at \$.31/liter (cost to Spire)	\$32,085	(b)	99,011
<u>TOTAL COST</u>	(a) Phosphorus \$ 531,073	(b) Boron \$ 536,051	
<u>TOTAL WATTS</u>	5,073,000	5,073,000	
<u>COST PER WATT</u>	\$0.105	\$0.106	

The throughput of the annealer is limited by the time required to load and unload a wafer, and to move the wafer through the required scanning pattern (Figure 8). Tentatively it is assumed that one-half second is sufficient to load or unload the wafer from the vacuum chuck, that each of the four annealing passes can be completed in one second, and that the sum of all movement perpendicular to the annealing scan direction can be completed in one second. The total time required is six seconds for a total throughput of 600 wafers per hour, matching the throughput of the ion implanter.

The linear speed of the wafer during annealing, assuming the scanning pattern in Figure 8, must be 10 cm/sec. The speed of the wafer in the x-direction must be twice that or 20 cm/sec, which is the top speed of the x-y table chosen for experimental work. The annealing pattern of overlapping pulses in Figure 8 suggests a beam width of 2 mm and a length of 30 mm, with 50% overlap and a pulse every time the wafer moves 1 mm. The repetition rate of the laser must be 100 Hz with an energy per pulse of 0.45 joules. This allows for a fluence of 0.75 J/cm^2 which is sufficient for annealing texture-etched material (Table 2.) A 50 watt laser should be sufficient for production.

From the initial technical results of this program (Section 2.2) and published results, either KrF or XeCl may be used in the excimer laser for annealing. The laser using KrF may be smaller for a fixed output (50 watts) as the use of this gas is more efficient than XeCl. However, the lifetime of a single gas fill is greater for XeCl than for KrF so the cost of gas in the krypton laser is greater. Which laser has the lower operating cost. The following calculation is based upon numbers furnished by Questek. We assume operation of the laser for three shifts per day, 8280 hours per year, the same assumed for the ion implanter.

ORIGINAL PAGE IS
OF POOR QUALITY

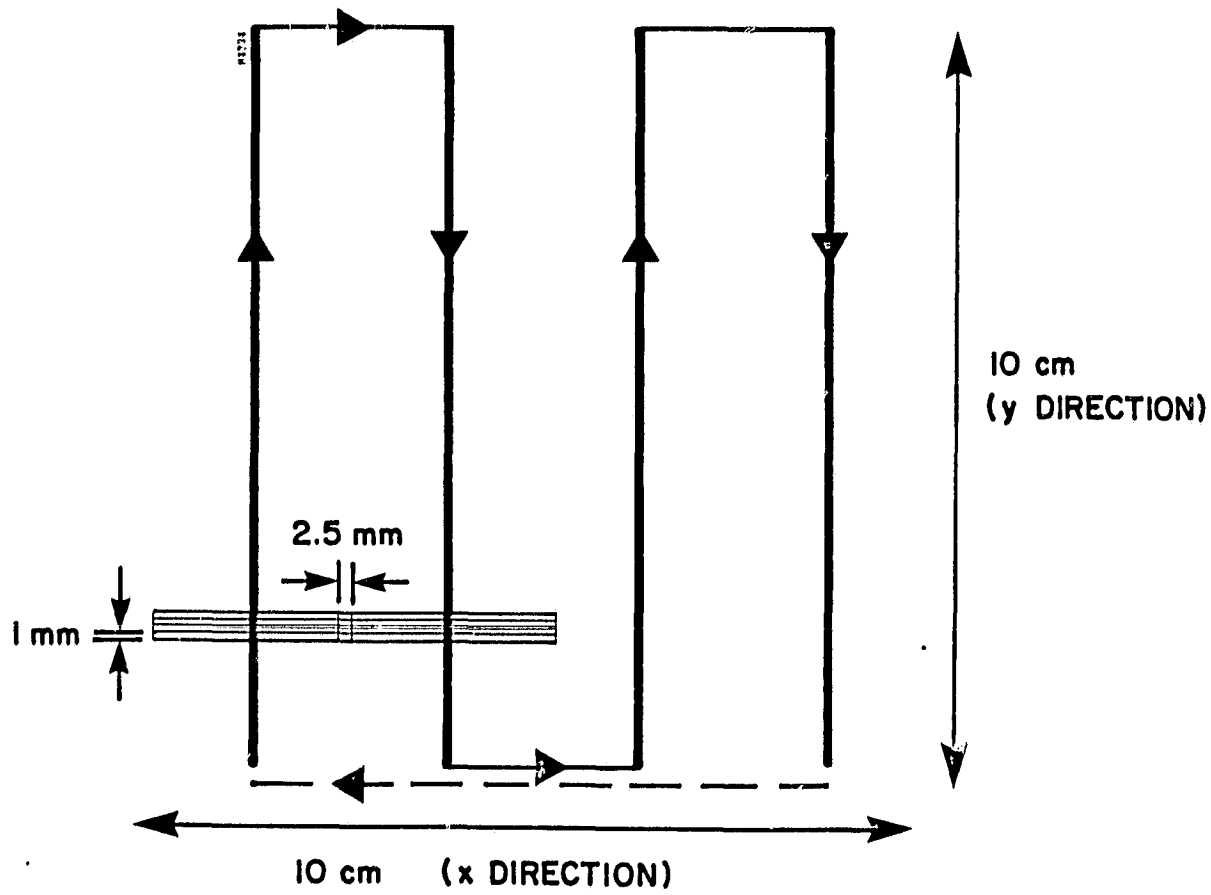


FIGURE 8. SCANNING PATTERN FOR ANNEALING A
100 cm² SQUARE WAFER

In addition to the cost of running the laser, the annealer has included, for either type of gas used, the following estimated common costs.

x-y Table and Controller	\$ 8,000
Cassette load/unload (kinetics)	\$10,000
Optics and Mountings	\$ 5,000
Miscellaneous Parts & Assembly	<u>\$25,000</u>
Total added price	\$48,000
Spare Parts (optics)	\$ 2,000 (Per shift per year)
Electricity	1 kw

PULSED EXCIMER LASER ANNEALING COST

	XeCl	KrF
EQUIPMENT PRICE x 0.59 (Includes \$48K non-laser parts and spares for 1 year)	\$ 110,625	\$ 84,075
FLOOR AREA 32 sq. ft. x \$136	\$ 4,400	\$ 4,400
DIRECT LABOR x 2.02 1/2 Operator \$5/hr 0.12 or 0.10 maintenance at \$10/hr 8280 hours/year	\$ 103,626	\$ 100,395
MATERIALS Spare parts Gas Electricity (\$0.10/kWhr)	\$ 80,500 \$ 52,009 \$ 4,968 6kW \$ 160,848	\$ 56,500 \$ 77,335 \$ 2,898 3.5kW \$ 159,978
TOTAL COST WATTS OUTPUT COST PER PEAK WATT	\$ 379,499 5,073,000 \$0.069/W _p	\$ 348,847 5,073,000 \$0.060/W _p

The costs to operate either laser, labor plus spare parts, plus gas, plus electricity, are nearly equal. The extra cost of gas for the KrF laser is compensated by the increased costs for spare parts for the XeCl laser. New technical advances which might extend gas life might favor the KrF laser. However, there is no clear cost differential at this time.

TABLE 3
PROCESS SEQUENCE COMPARISON
(5 MW Per Year Plant)

<u>Process Step</u>	<u>Yield</u>	<u>Value Added</u> (1980 \$/watt)	
		<u>Sample Process</u>	<u>Excimer Laser</u>
Clean	.994	.03	.0263
Dry	.999	.02	.0175
<u>Original</u>	<u>Excimer Laser</u>		
Diffuse Jcn	Implant Front		
Alum BSF	Implant Back	.973	.349
Clean	Anneal Back		
	Anneal Front		
Print Ag Back	.99	.09	.0788
Print Ag Front	.99	.09	.0788
Laser Cut	1.00	.07	.0613
Test and Sort	.950	.02	.0175
Cell Layup	1.00	.11	.0963
Prepare Materials	1.00	.17	.1488
Layup	.999	.13	.1138
Bond, Head & Vacuum			
To Module Layop	.998	.02	.0175
Trim Seal	.999	.03	.0263
Final Test	.990	.02	.0175
Pkg Module	.999	.05	.0438
Sub Total		1.00	.9370
<u>Input</u>			
<u>Silicon Substrate</u>		<u>1.91</u>	<u>1.670</u>
TOTAL		2.91	2.763
<u>Cost Savings</u>			<u>.147 per watt</u>

2.3.3 Process Sequence Comparison

The cost of a module using the baseline process is compared to that using the PELA process in Table 3. The key assumption is that the PELA process will result in 16% efficient cells, as opposed to 14% in the baseline process. This reduces the cost of all steps and the final module cost for PELA. A further reduction in cost of \$0.175/W_p is possible if the back implant is unnecessary in this low resistivity material. The baseline process requires the aluminum BSF because the n⁺ junction is diffused into both sides of the wafer initially. The ion-implanted, laser annealed junction is only on one side of the wafer and a BSF is not needed if the ink used in screen printing the back contact can make an ohmic contact to the silicon wafer directly.

2.4 OTHER TASKS

Task (I) (C) Demonstration of appropriateness of laser: No work has been performed on this task.

Task (I) (D) Demonstration of product: No work has been performed on this task.

SECTION 3

CONCLUSIONS AND RECOMMENDATIONS

The main objective of this research, the determination of whether or not pulsed excimer laser annealing (PELA) is an economical alternative method of fabricating silicon solar cells, will be decided entirely on the estimated achievable efficiency of the process in production. The cost per wafer of implementing this process maybe twice as great as the cost of the equivalent element in the baseline process, but significant savings are realized for even marginal improvements in cell efficiency.

The first set of experiments have shown that PELA is relatively insensitive to changes in processing parameters. It was shown that annealing is feasible at 248 nm wavelength, but there is no technical reason to choose between KrF or XeCl. Above some threshold value, which varies with surface preparation, the final cell efficiency did not change with a factor of two change in fluence. With a long focal length lens (25 cm) the exact position and/or orientation of the surface of a wafer within ± 0.050 inch did not affect the final cell results. Shunting due to metal coverage of annealed and non-annealed surface areas did not occur.

The maximum solar cell efficiency achieved by PELA was equal to that of the control, an ion implanted furnace annealed cell. We have not yet seen any evidence that PELA is better than this control process. However, the relative insensitivity of pulsed excimer laser annealing to many important process parameters implies that it has strong advantages over other pulsed annealing techniques such as Q-switched ruby or Nd:Yag lasers and pulsed electron beams.

SECTION 4

PLANNED WORK IN THE NEXT REPORTING PERIOD

The research program is on schedule (Figure 9). In the next quarterly reporting period work should be completed on annealing phosphorus implants, and about two-thirds complete on annealing boron and BF_3 implants with an excimer laser. The preliminary economic comparison is almost complete; input data for SAMICS analysis was submitted to JPL and the results of that calculation will complete that task.

Technically, annealing tests at 308 nm must be compared to the results presented in Table I. Further optimization of fluence and overlap parameters is needed for PELA of texture-etched material. The back contact of cells in Table I must be improved. Back contacts of sintered aluminum (400°C), alloyed aluminum (620°C) and PELA of boron implants will be compared to determine if implantation and PELA of BF_3 or equivalent is necessary in 1 to 2 ohm-cm p-type silicon.

A screen printer and a sintering furnace for making low cost screen printed contacts to solar cells have been ordered. The process should be tested on ion implanted, furnace annealed solar cells by September when experiments with PELA and screen printed contacts are expected to start.

ORIGINAL PAGE IS
OF POOR QUALITY

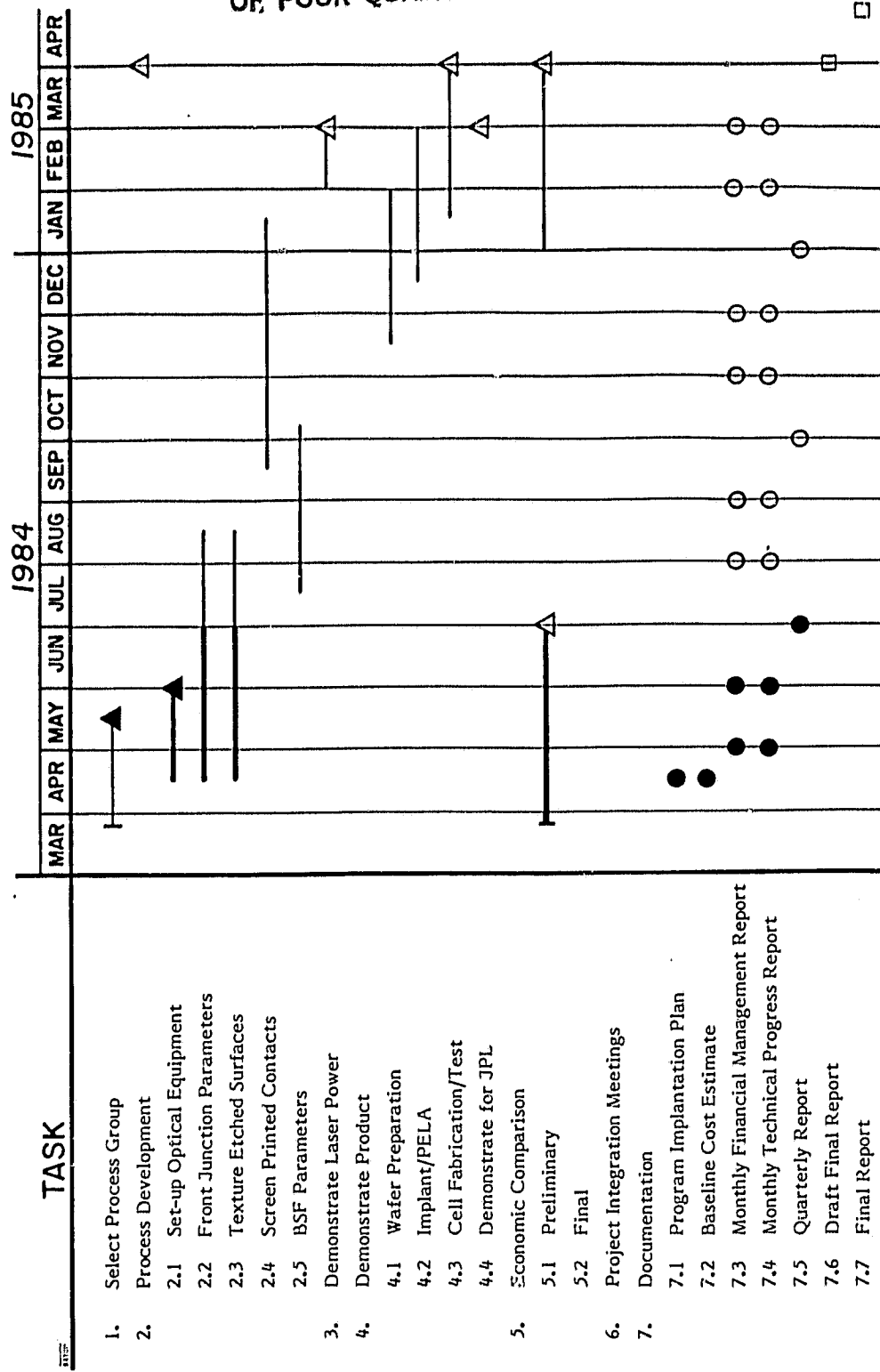


FIGURE 9. PROGRAM SCHEDULE

SECTION 5
REFERENCES

1. R.T. Young, G. A. Van Der Leeden, R.L. Sandstrom, R.F. Wood, and R.D. Westbrook, *Appl. Phys. Lett.* 43, 666 (1983).
2. M.B. Spitzer, S.P. Tobin and C.J. Keavney, *IEEE Trans. on Electron Dev.*, ED-31, 546 (1984).
3. Final report for JPL contract 954786 "Development of Pulsed Processes for the Manufacture of Solar Cells" (April 1979). Spire Corporation FR-10052. Final report for JPL contract 954289 "Development of Methods and Procedures for High Rate Low Energy Expenditure Fabrication of Solar Cells" (April 1976). Spire Corporation FR-10042.
4. R.T. Young, R.F. Wood, and W.H. Christie, *J. Appl. Phys.* 53 1178 (1982).
5. M.B. Spitzer and S.N. Bunker, *Appl. Phys. Lett.* 40, 976 (1982).
6. M.B. Spitzer, A.C. Greenwald, and R.G. Little, "Beam Processing Technology for Silicon Photovoltaics," in "Silicon Processing for Photovoltaics," edited by K.V. Ravi, to be published.
7. R.T. Young, J. Narayan, W.H. Christie, G.A. Van Der Leeden, D.E. Rothe, and R.L. Sandstrom in "Laser-Solid Interactions and Transient Thermal Processing of Materials" ed. J. Narayan, W.L. Brown, and R.A. Lemons, Material Research Society Proceedings v.13 (North-Holland, 1983) p. 401.
8. J.F. Young, J.S. Preston, H.M. Van Driel, and J.E. Sipe, *Phys. Review B* 127, 1155 (1983).